CHEMISTRY
A EUROPEAN JOURNAL

FULL PAPER

DOI: 10.1002/chem.201203506

Mechanism and Cellular Kinetic Studies of the Enhancement of Antioxidant Activity by Using Surface-Functionalized Gold Nanoparticles

Libo Du,[a] Siqingaowa Suo,[a] Guangqing Wang,[a] Hongying Jia,[a] Ke Jian Liu,*[b] Baolu Zhao,[c] and Yang Liu*[a]

Abstract: The enhanced antioxidant activity of surface-functionalized gold nanoparticles (AuNPs) synthesized by self-assembly has attracted great attention, but little is known about the mechanism behind the enhanced activity. To address this challenge, the antioxidant activity of Au@PEG3SA (i.e., surface-functionalization of spherical AuNPs with the antioxidant salvianic acid A) was used as an example to illustrate the mechanism of the enhanced activity. Evaluation of the antioxidant activity was performed in a radical-scavenging reaction between Au@PEG3SA and 2,2-diphenyl-1-picrylhydrazyl (DPPH) radical. As expected, the rate constant for the reaction of Au@PEG3SA with DPPH was about nine times greater than that for the salvianic acid A monomer. A comparative analysis of the spectral characteristics of Au@PEG3SA and the salvianic acid A monomer further imply that the enhancement of the antioxidative reaction kinetics may be ascribed to the variation in the transition state for the DPPH-radical scavenging reaction through π–π stacking interactions between and among adjacent groups on the surface of Au@PEG3SA. On the other hand, the kinetic enhancement of Au@PEG3SA on reactive-oxygen-species (ROS) scavenging can be observed in living cells and in vivo, which possibly provides new insight for the bioapplication of self-assembly of surface-functionalized AuNPs.

Keywords: antioxidants · cytotoxicity · gold · kinetics · nanoparticles · self-assembly

Introduction

The self-assembly of surface-functionalized gold nanoparticles (AuNPs) has been widely used in the field of materials science and life science due to their unique chemical and physical properties.[1–8] Among them, one of the most attractive phenomena is that the self-assembly of functional groups on the surface of AuNPs have the potential to significantly enhance the activity of the functional groups themselves. For example, Brown et al. have recently found that the anticancer activity of three platinum-tethered AuNPs against human lung cancer cell line A549 can be significantly improved.[6] Yet another study shows that amino-substituted pyrimidines, when self-assembled on the surface of AuNPs, can evidently enhance the antibacterial activities against multidrug-resistant clinical isolates without external sources of energy.[7] However, in most cases, the activity enhancement of the functional groups that are capped on the surface of AuNPs was usually ascribed to the high specific surface areas of AuNPs. Until 2007, there was almost no attention paid to the fact that the activity enhancement is probably related to an increase in the second-order rate constant for the reaction between the functional group that is self-assembled on the surface of AuNPs and other substrates in the solution.[8]

In the same study,[8] we demonstrated that the antioxidant activity of 6-hydroxy-2,5,7,8-tetramethylchroman-2-carboxylic acid (Trolox), a water-soluble analogue of Vitamin E, can be efficiently enhanced by the self-assembly of chromanol rings on the surface of AuNPs. After the self-assembly, the Vitamin E analogue possessed a radical scavenging activity eight times higher compared with the Trolox monomer. This paper was accompanied by an editorial commentary, emphasizing that the new idea of combining nanomaterial engineering with antioxidants represents a new concept for making better antioxidants without modifying the core structure of antioxidants.[9] Although the above study firstly demonstrated an enhancement on the reaction kinetics of functional groups by self-assembly of functional groups on the surface of AuNPs, however, there were still a few critical

[a] Dr. L. Du, S. Suo, G. Wang, Dr. H. Jia, Prof. Dr. Y. Liu
State Key Laboratory for Structural Chemistry
of Unstable Species, Center for Molecular Science
Institute of Chemistry, Chinese Academy of Sciences
Zhongguancun North First Street 2
100190 Beijing (P.R. China)
Fax:(+86) 106-255-93-73
E-mail: yliu@iccas.ac.cn

[b] Prof. Dr. K. J. Liu
College of Pharmacy, University of New Mexico
Albuquerque, NM 87131 (USA)
Fax: (+1) 505-272-0704
E-mail: kliu@salud.unm.edu

[c] Prof. Dr. B. Zhao
State Key Laboratory of Brain and Cognitive Science
Institute of Biophysics, Chinese Academy of Sciences
15 Datun Road, Chaoyang District, Beijing, 100101 (P.R. China)

Supporting information for this article is available on the WWW under http://dx.doi.org/10.1002/chem.201203506.

and vital challenges that must be overcome prior to its application in life science, especially when we intend to provide new types of antioxidant drugs. First of all, the mechanism for the kinetic effect of self-assembled nanoantioxidants should be elucidated to some extent through their structural characters. Thus one can reasonably design even higher efficiency nanoantioxidants, as well as some other nanoreactors; second, it is necessary to evaluate whether the kinetic enhancement of self-assembled nanoantioxidants on free-radical scavenging and inhibition of lipid peroxidation is maintained in living cells and in vivo. If applicable, our result would provide definitive experiment evidence for a biological application of the kinetic enhancement; third, the cytotoxicity of self-assembled nanoantioxidants should be taken into account before beginning the biological studies.

Meanwhile, to further check whether the phenomena of kinetic enhancement are universal for some other antioxidant-functionalized AuNPs, we synthesized PEG-coated AuNPs and then chose salvianic acid A (SA) to compose the self-assembled monolayer and antioxidative functional groups (SA is a natural polyphenol extracted from the dried root of *Salvia miltiorrhiza* and has been widely used in China, and to a lesser extent, in Japan, the United States, and other European countries for the treatment of cardiovascular and cerebrovascular diseases[11,12]). Next, the kinetic behavior of the radical-scavenging activity in vitro and in living cells was evaluated by means of stopped-flow analysis, laser-scanning confocal microscopic observation, and the thiobarbituric acid reactive substances (TBARS) assay, respectively. Additionally, the cytotoxicity of Au@PEG3SA was examined by using the methyl thiazolyl tetrazolium (MTT) method.

Results and Discussion

Synthesis and characterization of self-assembled nanoantioxidants (Au@PEG3SA): As shown in Figure S1 (the Supporting Information), PEG-coated AuNPs, that is, Au@PEG3, were synthesized by using a ligand-exchange method according to a similar procedure described previously.[12,13] Then, Au@PEG3 was covalently conjugated to salvianic acid A by an esterification reaction to produce Au@PEG3SA (Scheme 1). To confirm whether salvianic acid A had been successfully conjugated to the surface of AuNPs, the prepared nanoparticles were characterized by transmission electron microscopy (TEM), X-ray photoelectron spectroscopy (XPS), fourier transform infrared spectroscopy (FT-IR), and ultraviolet/visible spectroscopy (UV/Vis), respectively. The TEM image indicates that the Au@PEG3SA has an average size of 4.5 nm (Figure S1, the Supporting Information). The UV/Vis spectrum shows a characteristic absorbance peak at 286 nm, indicating the presence of salvianic acid A on the surface of AuNPs. Moreover, the surface plasmon resonance band is located at 521 nm (Figure S2, the Supporting Information) and in agreement with its average particle size.[14] Additionally, the FT-IR spectrum of Au@PEG3SA closely resembles that of salvianic acid A (see Figure S3, the Supporting Information). Together, these results provide clear evidence for the formation of salvianic acid A-conjugated AuNPs, and the representative chemical formula of Au@PEG3SA is derived as $Au_{1650}@PEG3_{776}DSS_{291}$, referring to our previous calculation.[8]

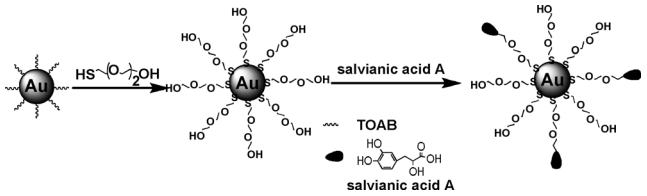

Scheme 1. Synthesis of salvianic acid A-functionalized AuNPs (Au@PEG3SA).

Assessment of the antioxidant activity by using the DPPH radical-scavenging assay: To evaluate the antioxidant activity of Au@PEG3SA, the radical scavenging profiles of Au@PEG3SA and authentic salvianic acid A were comparatively examined by using 2,2-diphenyl-1-picrylhydrazyl (DPPH) radical, which has been widely used to test the ability of compounds to act as free-radical scavengers.[15] As shown in Figure 1a, the time-dependent DPPH radical-scavenging data reveal a remarkable difference in reaction kinetics between Au@PEG3SA and salvianic acid A, and indicate that the self-assembly of PEGylated salvianic acid A group on the surface of AuNPs significantly enhances the DPPH radical-scavenging rate compared with the salvianic acid A monomer.

To quantitatively assess the distinction between Au@PEG3SA and salvianic acid A in the kinetics of their reactions with a DPPH radical, the rate constants for both reactions were determined by using the stopped-flow method.[16] Briefly, the stopped-flow experiments were conducted with a large excess concentration of salvianic acid A or Au@PEG3SA (0.1–1.0 mM), relative to the DPPH radical (40 μM), thus forcing the reactions to behave as pseudo-first order. Unless specified otherwise, the concentration of Au@PEG3SA represents the molar concentration of salvianic acid A groups. The dependence of the observed pseudo-first-order rate constant (k_{obs}) on the concentration of Au@PEG3SA and salvianic acid A is exhibited in Figure 1b. From the best-fitting slopes of the two lines, the rate constants of both reactions can be estimated to be $(65.3 \pm 1.65)\,M^{-1}s^{-1}$ and $(7.13 \pm 0.55)\,M^{-1}s^{-1}$, respectively. It can therefore be concluded that the rate constant for the reaction of Au@PEG3SA with the DPPH radical is over nine times greater than that for salvianic acid A, suggesting that Au@PEG3SA possesses a much greater free-radical-scavenging activity than the salvianic acid A monomer. These results support the conclusion that the antioxidant activity can be dramatically improved by the assembly of antioxidant groups on the surface of AuNPs.

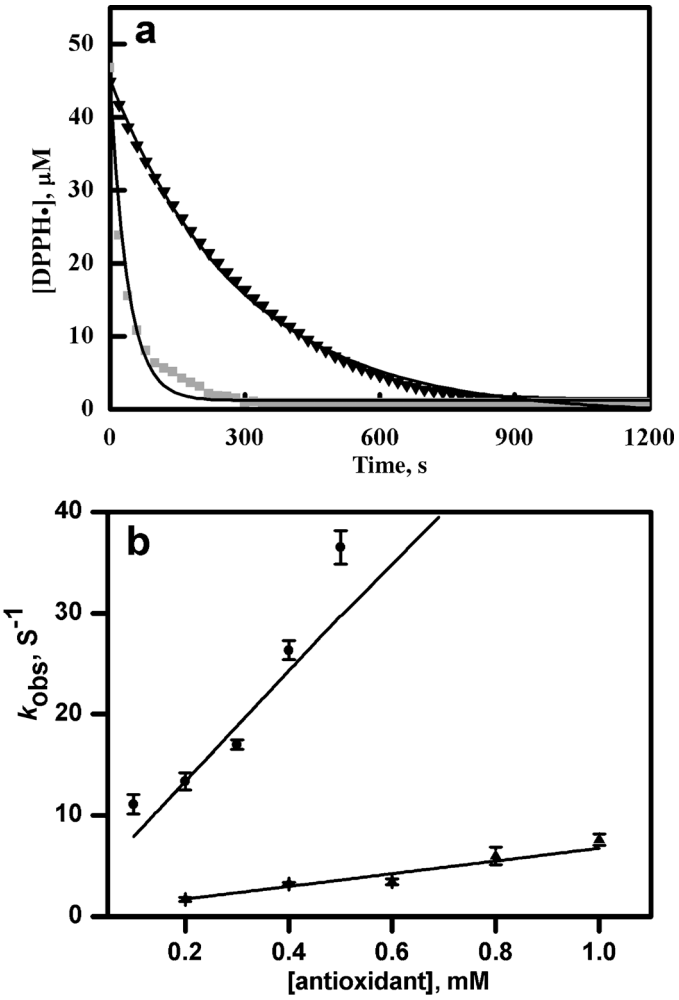

Figure 1. a) Decay of the DPPH radical in the presence of salvianic acid A (0.4 mM; black) and Au@PEG3SA (0.4 mM; gray). b) Plot of the pseudo-first-order rate constant (k_{obs}) versus the concentration of Au@PEG3SA (●) and salvianic acid A (▲). Conditions: [DPPH•] (45 μM L^{-1}) in methanol.

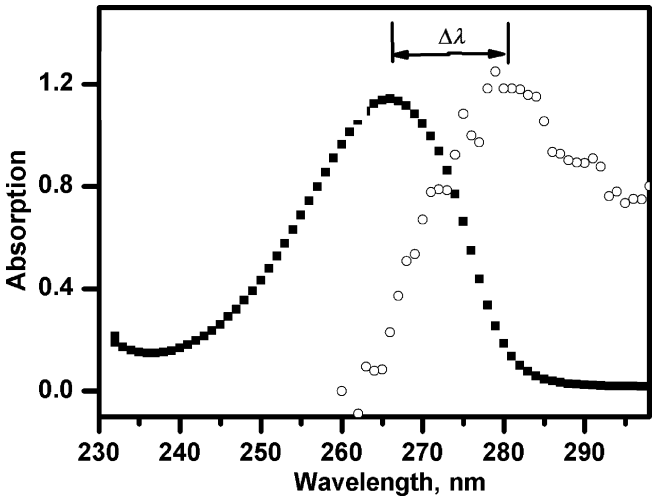

Figure 2. Normalized UV/Vis spectra of the salvianic acid A monomer (■) and Au@PEG3SA (○) in methanol.

The mechanism of enhanced antioxidant activity of Au@PEG3SA: Our previous study excluded that the enhancement of the antioxidant efficiency of nanoantioxidants is due to the direct participation of AuNPs in scavenging the DPPH radical.[8] However, to further explain why the assembly of phenolic groups on AuNPs could efficiently enhance the reaction kinetics of the nanoantioxidants, such as Au@PEG3SA, we comparatively analyzed the spectral differences between Au@PEG3SA and the salvianic acid A monomer that may be a potential cause of the kinetic behavior. As expected, Au@PEG3SA shows a considerable redshift (from 267 to 278 nm) of the maximum absorption as compared with the salvianic acid A monomer (Figure 2), probably indicating the existence of π–π stacking interactions between and among the adjacent phenolic groups coated on the surface of AuNPs. Pi stacking (also called π–π stacking) refers to attractive, noncovalent interactions between aromatic rings. Numerous previous studies have demonstrated that the π–π stacking alignment between aromatic compounds can cause an obvious redshift of UV/Vis spectrum.[17] For example, the UV/Vis absorption spectrum of porphyrin derivatives assembled on the AuNPs showed an apparent redshift larger than that of porphyrin-free form, which provides direct evidence for the existence of π–π stacking alignment on the surface of AuNPs.[18] On the other hand, it has been reported that the aromatic stacking of the adjacent groups may change the dynamic structure and the energy of the transition state and ultimately results in a change in the reaction pathway and variation of the reaction kinetics.[19–22] More evidence for the stacking alignment can be revealed from the redshift in FT-IR spectrum; a widely used tool in characterizing the self-assembled functional materials.[23–25] As illustrated in Figure S4 (the Supporting Information), the C=C and C–H stretching vibration frequencies of Au@PEG3SA were redshifted by about 13 cm^{-1} (from 1579 to 1592 cm^{-1}) and 8 cm^{-1} (from 881 to 889 cm^{-1}), respectively, compared with the published FT-IR spectrum of the salvianic acid A monomer.[26] These redshifts indicate the existence of π–π stacking between or among adjacent phenolic groups on the surface of AuNPs, which possibly can be used to explain the enhanced kinetic behavior of the self-assembled nanoantioxidants and thus enable the understanding of a new approach in the design of more efficient nanoantioxidants.

Kinetic studies of the radical-scavenging activity of Au@PEG3SA in living cells and in vivo: The kinetic antioxidant exerts its antioxidant activity mainly through scavenging oxygen-centered free-radicals and other reactive-oxygen species (ROS). As one of the commonly used models of ROS generation, *t*BuOOH is used to stimulate the formation of free radicals through microsomal cytochrome P450.[27–28] To further examine whether the enhanced kinetic scavenging effect of Au@PEG3SA on ROS can be observed in living cells, we comparatively detected the time-depend-

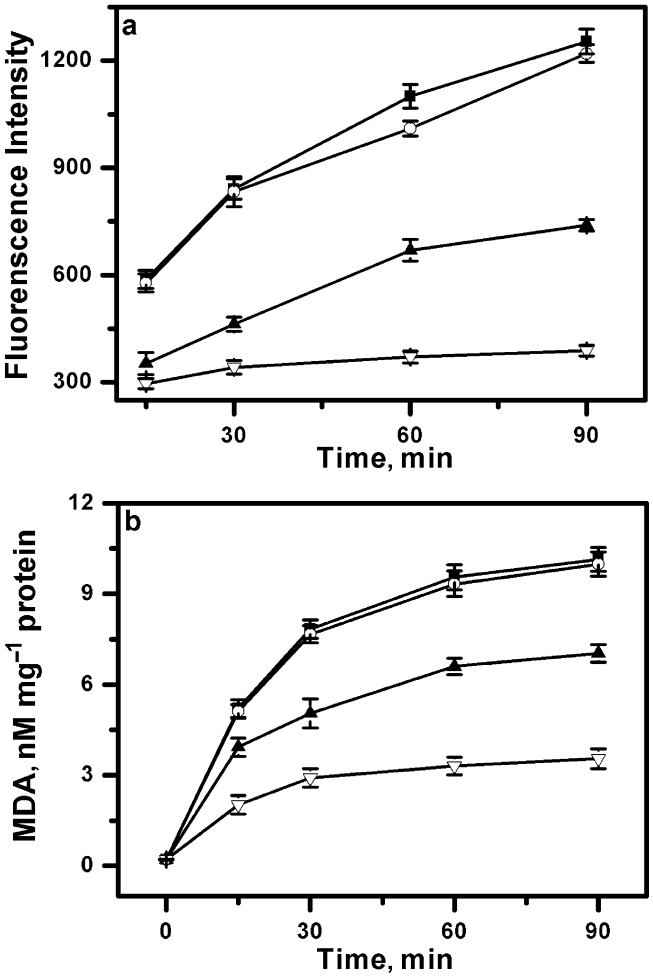

Figure 3. a) Time-dependent inhibitory effects of Au@PEG3 (○), Au@PEG3SA (▽), and salvianic acid A (▲) on the production of intracellular reactive oxygen species in RAW 264.7 cells. ■ = *t*BuOOH. b) Time-dependent protecting effect of Au@PEG3, salvianic acid A monomer, and Au@PEG3SA on oxidative stress in RAW 264.7 cells (MDA is an oxidative-stress marker). RAW 264.7 cells were pre-incubated for 12 h with Au@PEG3 (470 μM, the concentration of AuNPs), Au@PEG3SA (80 μM), or salvianic acid A (80 μM), and then exposed to 100 μM of *t*BuOOH for 20 min. Values exhibit mean ±SD and each experiment was performed in triplicate. ■ = *t*BuOOH; ○ = *t*BuOOH/Au@PEG3; ▲ = *t*BuOOH/salvianic acid A; ▽ = *t*BuOOH/Au@PEG3SA.

ent profiles of intracellular ROS in RAW 264.7 cells in the presence of Au@PEG3SA and the salvianic acid A monomer, respectively. The ROS production was initiated with *t*BuOOH (100 μM) and detected by using 2′,7′-dichlorodihydrofluorescein diacetate (DCF-DA) fluorescence staining methods (Figure S5, the Supporting Information). As shown in Figure 3a, the fluorescence level of *t*BuOOH-treated cells increased in a time-dependent manner, with a successive increase up to 90 min. For cells pretreated with salvianic acid A, the fluorescent intensity was evidently decreased during the first 60 min and then increased much more slowly than before, suggesting that salvianic acid A can inhibit the cellular ROS production. Most importantly, compared with the salvianic acid A monomer, the fluorescence intensity was kept to a very low level throughout the 90 min in the presence of Au@PEG3SA, implying that Au@PEG3SA can much more efficiently scavenge the *t*BuOOH-induced intracellular ROS. This result suggests that the enhanced kinetic effect of the antioxidant-functionalized AuNPs in ROS scavenging is maintained in living cells.

Inside a living cell, *t*BuOOH-induced oxygen-centered free-radicals can easily abstract an electron from polyunsaturated fatty acid (LH) to give rise to a carbon-centered lipid radical (L$^{\bullet}$), which further reacts with molecular oxygen to produce a lipid peroxyl radical (LOO$^{\bullet}$). If the resulting LOO$^{\bullet}$ is not rapidly reduced by endogenous antioxidants, the free-radical chain reaction will be initiated, leading to lipid peroxidation. Malonyldialdehyde (MDA), a three-carbon dialdehyde, is produced as an end product of polyunsaturated lipid-peroxidation and generally regarded as a biomarker to measure the level of lipid peroxidation.[29] Thus, to compare the dynamic protecting effects on lipid peroxidation, the time-dependent MDA contents in RAW 264.7 cells were measured using a thiobarbuturic acid (TBA) method in the presence of the Au@PEG3SA and salvianic acid A, respectively. The lipid peroxidation was initiated by *t*BuOOH. As shown in Figure 3b, the MDA level of control group (*t*BuOOH only) was increased in a time-dependent manner following incubation with *t*BuOOH. When RAW 264.7 macrophage cells were pretreated with Au@PEG3SA, the MDA level was much lower and increased much more slowly, indicating that the cellular lipid-peroxidation was maintained at a very low level, that is, the presence of Au@PEG3SA eliminates 70% of the total lipid-peroxidation. In comparison to Au@PEG3SA, the salvianic acid A monomer only inhibited about 30% of the total lipid-peroxidation.

Taken together, the cellular mechanism of enhanced antioxidant activity for Au@PEG3SA in living cells might be speculated as follows: Cellular lipid-peroxidation usually refers to a free-radical-related process that could be suppressed by endogenous antioxidants, such as Vitamin E and CoQ10,[30] because the rate constant for the propagation step of lipid peroxidation ($\approx 10\,M^{-1}s^{-1}$) is far less than that for the lipid radical-scavenging reaction by Vitamin E ($\approx 10^4\,M^{-1}s^{-1}$).[31] However, due to the limited amount of antioxidants in cell membranes, once the antioxidants are depleted, lipid peroxidation would take place. As a result, supplement exogenous antioxidants would protect against lipid peroxidation. The salvianic acid A monomer plays a role similar to Vitamin E in inhibiting the lipid peroxidation through competitive reactions between propagation reactions and the lipid radical-scavenging reaction. Compared with the salvianic acid A monomer, Au@PEG3SA can more rapidly react with *t*BuOOH-initiated radicals, and as a result, more effectively inhibit the propagation step of lipid peroxidation, thus dramatically reducing the MDA content in cells. Therefore, the observation of enhanced antioxidant activity of Au@PEG3SA in macrophage cells could be attributed to its higher reaction rate constant relative to that of the salvianic acid A monomer.

On the other hand, previous studies have proved that antioxidant treatment could reduce oxidative damage in *C. elegans*.[32,33] The oxidative stress can be initiated in *C. elegans* by exposure to paraquat, which is an in vivo model of free-radical-induced oxidative damage. To further examine the enhanced kinetic-scavenging effect of Au@PEG3SA on ROS in an in vivo model system, the time-dependent signal intensities of ROS were tested in the presence of Au@PEG3SA and the salvianic acid A monomer, respectively (as shown in Figure 4). After 12 h of incubation with paraquat, the accumulation of ROS within the cells of individual *C.elegans* was measured by using DCF-DA. As expected, our result shows that paraquat led to increased ROS accumulation in a time-dependent manner. When *C.elegans* were pretreated with Au@PEG3SA, the fluorescence level only increased slightly within the first 2 h, before reaching a plateau. In fact, most of the fluorescence signal (above 85%) could be quenched after 4 h incubation with Au@PEG3SA, indicating that ROS generated by paraquat were mostly scavenged. In comparison with the nanoantioxidant, the salvianic acid A monomer was able to scavenge roughly half the amount of ROS during the whole incubation period. All these results demonstrate that the nanoantioxidants have an enhanced kinetic-scavenging effect on ROS in vivo, which would likely slow the oxidative damage to worms. This finding is the first demonstration that the antioxidant-functionalized AuNPs in ROS scavenging are maintained in an in vivo model system.

Cytotoxicity assay on mammalian cells: To assess the biocompatibility of Au@PEG3SA, the cytotoxicity of Au@PEG3SA under in vitro conditions was evaluated by using the MTT assay. Considering that macrophages are the first line of defense in the immune system and act as scavengers against foreign agents through phagocytosis, the cell viability of macrophage cell line RAW 264.7 was measured in the presence of Au@PEG3SA.[34] Figure 5 shows the cell viability data after 24 h of incubation with an increasing concentration of Au@PEG3SA. After incubation for 24 h with Au@PEG3SA, the cell viability was more than 90%, even at 120 μM, which is probably a much higher concentration than encountered in vivo.[35] As a result, salvianic acid A-functionalized AuNPs would present an efficient antioxidant with low cytotoxicity for application in biological systems.

Conclusion

A new gold nanoparticle-based salvianic acid A, that is, Au@PEG3SA, was synthesized by using a layer-by-layer self-assembly method. The DPPH radical-scavenging assay indicates that the rate constant for the reaction of the DPPH radical with Au@PEG3SA was about nine times higher than that with salvianic acid A monomer. Meanwhile, we have also demonstrated that the mechanism for the kinetic enhancement of Au@PEG3SA was probably due to variation in the transition state for the DPPH radical-scavenging reaction, possibly through the π–π stacking interactions among adjacent phenolic groups that are located on the surface of AuNPs. Another particularly striking finding was the dramatic increase in the reaction kinetics for the ROS scavenging process in living cells, as well as in vivo,

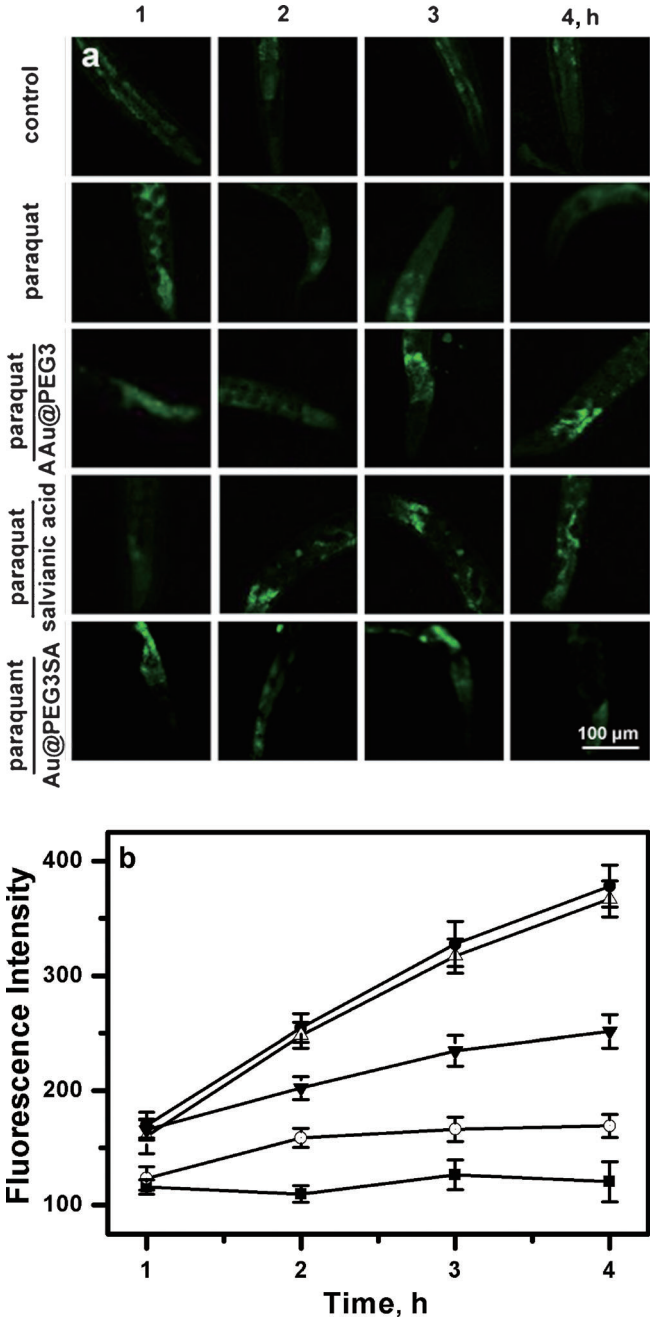

Figure 4. Time-dependent inhibitory effects of Au@PEG3, Au@PEG3SA, and salvianic acid A on the production of reactive oxygen species in *C.elegans*. *C.elegans* were pre-incubated for 12 h with Au@PEG3 (470 μM, the concentration of AuNPs), Au@PEG3SA (80 μM), or salvianic acid A (80 μM), and then exposed to paraquat (400 μM) for 4 h. a) The fluorescence intensity in *C.elegans* was monitored by confocol microscopy. The statistical analysis of the fluorescence obtained from (a) was profiled in (b). The values exhibit mean ±SD and each experiment was performed in triplicate. ■=control; ●=paraquat; △=Au@PEG3 pretreated; ▼=salvianic acid A pretreated; ○=Au@PEG3SA pretreated.

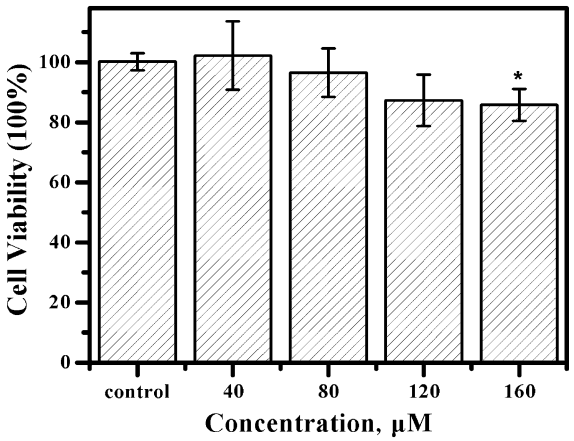

Figure 5. RAW 264.7 cell viability after 24 h of exposure to various concentrations of Au@PEG3SA. Data are the mean ±SEM results of six measurements from three independent experiments. *$P < 0.05$ versus control.

which is the underlying mechanism leading to a kinetic enhancement of cellular antioxidant status. Perhaps more importantly, our study provides a new strategy for the design and fabrication of highly efficient surface-functionalized AuNPs, as well as exhibiting their potential applications in biology and medicine.

Experimental Section

Synthesis of salvianic acid A-functionalized gold nanoparticles (Au@PEG3SA): Au@PEG3 was synthesized by treating a suspension of tetraoctylammonium bromide (TOAB)-stabilized gold nanoparticles with thiol 2-(2-(2-mercaptoethoxy)ethoxy)ethanol in dichloromethane. The resulting suspension was stirred under N_2 for 1 day. After removing the solvent, the slurry of the crude Au@PEG3 nanoparticles was redissolved and purified by column chromatography by using sephadex LH-20 (methanol eluent). Then, EDC (34 mg 0.18 mm) and DMAP (21.9 mg 0.18 mm) were added to a solution of Au@PEG3 (20 mg) and salvianic acid A in anhydrous DMF (10 mL) with stirring for 1 h at 0 °C and then overnight at room temperature. The solution was evaporated and subsequent purification by column chromatography using sephadex LH-20 (methanol eluent) to remove the byproducts and excess salvianic acid A. The pure nanoparticles (Au@PEG3SA) were stored as dry powder at −20 °C until use.

Kinetic measurements of DPPH radical-scavenging by using a stopped-flow technique: The kinetic data were obtained with a stopped-flow spectrophotometer (Hitach UV3310) by mixing equal volumes of the DPPH radical (0.5 mM) and Au@PEG3SA or salvianic acid A in a solution of methanol under a nitrogen atmosphere.[36] The time between mixing the two solutions and recording the first data point was 20 ms. The reaction was monitored by single wavelength detection attached to the stopped-flow spectrophotometer. All measurements were performed at −(30±0.5) °C.

Intracellular ROS determination: The generation of intracellular ROS was detected using the fluorescence probe DCF-DA. Cells were plated in a 96-well plate (1×10^5 cells per well). After 24 h, cells were treated with salvianic acid A or Au@PEG3SA for 12 h. After the medium was washed off, DAF-DA and *t*BuOOH were added to the cells. The plate were then incubated at 37 °C for 1 h. Hereafter, the cells were washed three times with PBS (0.1 M pH 7.4) to remove the excess probe. The fluorescence intensity was measured at an excitation wavelength of 488 nm and an emission of 515 nm by using a fluorescent mutilabel counter. The relative amount of intracellular ROS production was expressed as the fluorescence ratio of the treatment to control.

Analysis of the level of lipid hydroperoxides: The thiobarbituric acid reactive substance (TBARS) contents were measured according to the original method of Buege and Aust[37] with some modifications. Briefly, cells were plated in on petri dishes. After 24 h, cells were treated with salvianic acid A, or Au@PEG3SA for 12 h. After the medium was washed off, *t*BuOOH was added to the cells. The plates were then incubated at 37 °C for 4 h. Subsequently, the freshly prepared TBA reagent was added (750 μL from a stock prepared as follows: 2-thiobarbituric acid (200 mg) solubilized in sodium hydroxide (2 M, 9 mL), pH adjusted to 7.4 with 7% perchloric acid, and deionized water added to 25 mL; two volumes of this solution were mixed with one volume of 7% perchloric acid to use as the TBA reagent). The caps of the tubes were tightly screwed and the tubes were placed in a boiling bath for 10 min. After cooling down to room temperature, *n*-butanol (1.5 mL) was added to each tube, thoroughly mixed and centrifuged for 15 min at 3000 g. After centrifugation, the supernatant was used to measure fluorescence in a Hitach FL-3310. A standard run was included in each batch, prepared from a solution of tetraethoxypropane (2.5 mM) to generate MDA (final concentrations of MDA in the standards were 0.5, 1.5, 2.5, and 3.5 μM).

Accumulation of the reactive oxygen species in *C.elegans*: The nematodes were cultured as described in literature.[38] On day 5, *Caenorhabditis elegans* (*C.elegans*, wild-type N2 strain) was treated with salvianic acid A (0.5 mM) or Au@PEG3SA (0.5 mM) and preceded for 2 days, then washed extensively. The worms were incubated with paraquat (0.4 mM) for 4 h, and then washed three times with M9 buffer. Subsequently, the worms were transferred to Hank's solution (1 mL) containing DCF-DA (10 μM; Sigma-aldrich) and incubated for 30 min at 20 °C. To determine the fluorescence of DCF, fixed nematode samples were subjected to Olympus laser-scanning confocal microscopy (excitation at 488 nm and emission at 510 nm). The relative fluorescence of the whole body was determined densitometrically by using the Olympus software.

Acknowledgements

This project was supported by the National Natural Science Foundation of China (No. 91227122 and 21005082) and the Knowledge Innovation Program (Grant No. KJCX2-EW-H01) of the Chinese Academy of Sciences.

[1] C. Kim, S. S. Agasti, Z. J. Zhu, L. Isaaces, V. M. Rotello, *Nat. Chem.* **2010**, *2*, 962–966.
[2] L. Vigderman, P. Manna, E. R. Zubarev, *Angew. Chem. Int. Ed.* **2012**, *51*, 636–641.
[3] B. N. Zope, D. D. Hibbitts, M. Neurock, R. J. Davis, *Science* **2010**, *330*, 74–78.
[4] G. Pelossof, R. Tel-Vered, X. Q. Liu, I. Willner, *Chem. Eur. J.* **2011**, *17*, 8904–8912.
[5] A. C. Templeton, M. J. Hostetler, C. T. Kraft, R. W. Murray, *J. Am. Chem. Soc.* **1998**, *120*, 1906–1911.
[6] S. A. Brown, P. Nativo, J. A. Smith, D. Stirling, P. R. Edwards, B. Venugopal, D. J. Flint, J. A. Plumb, D. Graham, N. J. Wheate, *J. Am. Chem. Soc.* **2010**, *132*, 4678–4684.
[7] Y. Y. Zhao, Y. Tian, Y. Cui, W. W. Liu, W. S. Ma, X. Y. Jiang, *J. Am. Chem. Soc.* **2010**, *132*, 12349–12356.
[8] Z. Nie, K. J. Liu, C. J. Zhong, L. F. Wang, Y. Yang, Q. Tian, Y. Liu, *Free Radical Biol. Med.* **2007**, *43*, 1243–1254.
[9] H. Y. Yin, *Free Radical Biol. Med.* **2007**, *43*, 1229–1230.
[10] L. M. Zhou, Z. Zou, M. S. S. Chow, *J. Clin. Pharmacol.* **2005**, *45*, 1345–1359.
[11] Y. G. Cao, J. G. Chai, Y. C. Chen, J. Zhao, J. Zhou, J. P. Shao, C. Ma, X. D. Liu, X. Q. Liu, *Br. J. Pharmacol.* **2009**, *157*, 482–490.

[12] G. Prencipe, S. M. Tabakman, K. Welsher, Z. Liu, A. P. Goodwin, L. Zhang, J. Henry, H. J. Dai, *J. Am. Chem. Soc.* **2009**, *131*, 4783–4787.
[13] M. Brust, D. Bethell, D. J. Schiffrin, C. J. J. Kiely, *Adv. Mater.* **1995**, *7*, 795–797.
[14] L. Valgimigli, J. T. Banks, K. U. Ingold, J. Lusztyk, *J. Am. Chem. Soc.* **1995**, *117*, 9966–9971.
[15] B. A. Wagner, G. R. Buettner, C. P. Burns, *Biochemistry* **1994**, *33*, 4449–4453.
[16] W. L. Lin, C. J. Wang, Y. Y. Tsai, C. L. Liu, J. M. Hwang, T. H. Tseng, *Arch. Toxicol.* **2000**, *74*, 467–472.
[17] J. K. Klosterman, Y. Yamauchi, M. Fujita, *Chem. Soc. Rev.* **2009**, *38*, 1714–1725.
[18] L. Zhang, X. Q. Li, J. Mu, *Coll. Surf. A: Physicochem. Eng. Aspects* **2007**, *302*, 219–224.
[19] S. Catak, M. D'hooghe, N. D. Kimpe, M. Waroquier, V. V. Speybroeck, *J. Org. Chem.* **2010**, *75*, 885–896.
[20] M. C. Foti, C. Daquino, I. D. Mackie, G. A. DiLabio, K. U. Ingold, *J. Org. Chem.* **2008**, *73*, 9270–9282.
[21] W. Versées, S. Loverix, A. Vandemeulebroucke, P. Geerlings, J. Steyaert, *J. Mol. Biol.* **2004**, *338*, 1–6.
[22] T. W. Yao, L. B. Du, Y. Yang, Y. C. Xu, H. Y. Jia, Y. Liu, *Chem. J. Chin. Univ.* **2009**, *30*, 1431–1433.
[23] N. Sandhyarani, T. Pradeep, *J. Mater. Chem.* **2000**, *10*, 981–986.
[24] S. Masuda, K. Hasegawa, A. Ishii, T. A. Ono, *Biochemistry* **2004**, *43*, 5304–5313.
[25] W. Z. Wang, M. Pitonak, P. Hobza, *ChemPhysChem* **2007**, *8*, 2107–2111.
[26] http://202.127.145.134/scdb/(Chemistry Database, Chinese Academy of Sciences).
[27] M. J. Davies, *Biochem. J.* **1989**, *257*, 603–606.
[28] A. G. Pirinccioglu, D. Gokalp, M. Pirinccioglu, G. Kizil, M. Kizil, *Clin. Chem.* **2010**, *43*, 1220–1223.
[29] F. Nielsen, B. B. Mikkelsen, J. B. Nielsen, H. R. Andersen, P. Grandjean, *Clin. Chem.* **1997**, *43*, 1209–1214.
[30] B. Halliwell, *Nutr. Rev.* **2009**, *52*, 253–265.
[31] G. R. Buettner, *Arch. Biochem. Biophys.* **1993**, *300*, 535–543.
[32] M. Bartneck, H. A. Keul, Z. K. Gabriele, J. Groll, *Nano Lett.* **2010**, *10*, 59–63.
[33] A. Kampkötter, C. G. Nkwonkam, R. F. Zurawski, C. Timpel, Y. Chovolou, W. Watjen, R. Kahl, *Toxicology* **2007**, *234*, 113–123.
[34] H. Ye, B. Ye, D. Wang, *Neurobiol. Learn. Mem.* **2008**, *90*, 10–18.
[35] H. J. Jin, *J. Chin. Med.* **1978**, *3*, 180–183.
[36] K. Mukai, A. Tokunaga, S. Itoh, Y. Kanesaki, K. Ohara, S. Nagaoka, K. Abe, *J. Phys. Chem. B* **2007**, *111*, 652–662.
[37] J. A. Buege, S. D. Aust, *Methods Enzymol.* **1978**, *52*, 302–310.
[38] WormBook, (Ed.:T. Stiernagle), The *C.elegans* Research Community, WormBook, doi/10.1895/wormbook.1.101.1.

Received: October 2, 2012
Published online: December 11, 2012

